# EVALUATION OF THE EFFECTS OF SKULL DEFLECTION ON BRAIN TISSUE RESPONSE USING FINITE ELEMENT SIMULATION

**Derek A. Jones, MS**
Virginia Tech-Wake Forest University Center for Injury Biomechanics, Winston-Salem, NC, USA
Wake Forest School of Medicine, Winston-Salem, NC, USA

**Jillian E. Urban, PhD**
Virginia Tech-Wake Forest University Center for Injury Biomechanics, Winston-Salem, NC, USA
Wake Forest School of Medicine, Winston-Salem, NC, USA
Clinical and Translational Science Institute, Winston-Salem, NC, USA

**Ashley A. Weaver, PhD**
Virginia Tech-Wake Forest University Center for Injury Biomechanics, Winston-Salem, NC, USA
Wake Forest School of Medicine, Winston-Salem, NC, USA

**Joel D. Stitzel, PhD**
Virginia Tech-Wake Forest University Center for Injury Biomechanics, Winston-Salem, NC, USA
Wake Forest School of Medicine, Winston-Salem, NC, USA

Paper Number 17-0414

## ABSTRACT

Traumatic brain injuries (TBIs) remain a large public health concern, with an estimated 2.8 million people in the United States alone sustaining a TBI annually, of whom 56,000 die. Despite the development of finite element (FE) models of the head, the implications of skull deflection on the risk of brain injury in blunt trauma is not well understood. There is currently a lack of injury metrics which quantify skull deflection; therefore, the objective of this study was to replicate experimental head impacts using the head from the Global Human Body Models Consortium 50th percentile male occupant model (GHBMC M50-O v4.5), develop a skull deflection injury metric, and evaluate the relationship between the skull deflection and tissue-based brain strain.

Three experimental test series were replicated using simulation techniques (Allsop, 1991; Cormier, 2011; Yoganandan, 1995). During each simulation, every brain element's strain tensors were output at 0.1 ms intervals. Similarly, the inner skull surface nodal displacements with respect to the head center of gravity were output at 0.1 ms intervals.

The brain elements were then grouped based on proximity to the impact site to define coup and contre-coup regions of interest (ROIs). A maximum skull deflection metric was developed for skull deflection characterization. Correlations between the skull deflection injury metric and coup ROI elemental strain measures were evaluated. Differences in the distribution of coup and contre-coup strain within single impacts were evaluated.

Nine experimental tests were simulated in this study. Input kinetic energy, impactor geometry, boundary conditions, and impact location from the respective experimental test were replicated in each simulation. Skull deflection ranged from 1.24-4.98 mm. 95th percentile coup and contre-coup maximum principal strains ranged from 0.02-0.08 and 0.008-0.048, respectively. Coup strain was positively correlated to the skull deformation metric. There were statistically significant differences between coup and contre-coup 95th percentile maximum principal strain.

Replicating cadaveric testing of heads allows for more in depth analysis into brain injury metrics that are unable to be studied from PMHS alone. Specifically, shape profiles of inner skull deformation were able to be characterized and compared to brain tissue response. A positive linear relationship was found between the skull deformation metrics and underlying brain strain, which is the likely source for focal brain injury. Thus, the skull deformation metric developed in this study will lead to a better understanding of the mechanistic relationship between skull deformation and head injury.

## INTRODUCTION

Approximately 2.8 million people in the United States sustain a traumatic brain injury (TBI) each year, 56,000 of whom die [1]. Furthermore, the annual economic cost of TBI in the United States is estimated to be $60 billion [2]. Motor vehicle crashes (MVCs) continue to be the third largest contributor to TBI related deaths [1]. Significant research has been conducted through the years to decipher the exact cause of brain injury including animal, cadaver, and finite element (FE) experiments [3-11]. These experiments have contributed to many theories regarding the mechanism of brain injury, however it is generally agreed upon that strain is likely the largest contributing factor [12]. Brain strains primarily develop as the result of rotation of the head at high rates of speed. This is due to the bulk modulus of brain tissue being approximately six orders of magnitude larger than the shear modulus resulting in deformation of tissue being more easily produced through deviatoric forces compared to dilatation forces [13, 14]. However, it has been demonstrated that in nearly every head injury in motor vehicles, the occupant sustained head contact and not merely kinematic rotation of the head through whiplash type effects [15-18]. Thus, blunt trauma to the head is a critical mechanism for sustaining head trauma and the scalp and skull are responsible for transmitting load to the brain. Furthermore, it has been shown that localized bending of the skull with or without fracture may cause localized or "focal" brain injuries such as intraparenchymal contusions or hemorrhage in extra-axial spaces [5].

Though it has been shown that the skull is the primary transmitter of energy to the brain and that contact location may affect injury location, much of the work in the field of FE modeling has been completed with models that are equipped with rigid skulls [14, 19]. These have advanced the body of knowledge and, indeed, provide perspective into the brain injury risk in various circumstances, but are likely missing a critical component of injury risk associated with skull deformation and localized strain [20]. As a result, the exact relationship between strain and skull deformation is unknown.

The purpose of this study is to elucidate the relationships between skull deformation, impactor geometry, kinetic energy, and brain strain in coup and contre-coup regions of the brain using the head from the Global Human Body Models Consortium (GHBMC) 50th percentile male occupant v4.5 [21, 22]. Specifically, this study is conducted in the absence of head rotational velocity, which is known to be a large contributor to diffuse strain distribution.

## METHODS

In order to investigate the relationships between skull deformation, impactor geometry, kinetic energy, and brain strain, a selection of physical cadaveric tests from the literature were chosen for FE simulation. The tests chosen for simulation encompassed various impact locations on the head and included temporo-parietal, parietal, frontal, occipital and vertex impacts. The original tests were conducted for the purpose of understanding skull fracture, and included boundary conditions that prevented head translational or rotational kinematics. These impacts ranged from 14.06 to 110.94 J in kinetic input energies and used multiple impactor geometries including cylindrical, rectangular, and spherical impactors [23-25]. A summary of the tests can be found in Table 1.

The head of the GHBMC M50-O v4.5 head model was transected from the remainder of the body at the occipital condyles. The distal ends of the head flesh were tied together using a constrained nodal rigid body. Physical test boundary conditions were recreated for each. In the Yoganandan impact simulations, the same boundary conditions were used for each impact regardless of impact location. The inferior portion of the skull and jaw were fixed in place. In the Cormier frontal impact simulation, and in both Allsop impacts, nodes of the skull on the contralateral side of head with respect to the impact location were held in space. Simulation termination times were chosen on a simulation by simulation basis such that the impactor was in the rebound phase at the end of the simulation. Element erosion to simulate fracture in the GHBMC M50 model's skull was turned off [26].

During each simulation, the GHBMC brain elements were set to export stress and strain data at 10 kHz frequency. The relative displacement of each node on

**Table 1. Experimental impact parameters for simulation boundary conditions [23-25].**

| Literature | Impactor Geometry | Test # | Impact Location | Impactor Velocity (m/s) | Impactor Mass (kg) | Impactor Kinetic Energy (J) |
|---|---|---|---|---|---|---|
| Allsop (1991) | Rectangular Plate | - | Parietal | 4.3 | 12 | 110.94 |
| | Circular Plate | - | Temporo-Parietal | 2.7 | 10.6 | 38.64 |
| Yoganandan (1995) | Hemispherical | 7 | Vertex | 7.2 | 1.2137 | 31.46 |
| | | 8 | Occipital | 7.1 | 0.9328 | 23.51 |
| | | 9 | Vertex | 7.6 | 1.3850 | 40.00 |
| | | 10 | Frontal | 7.3 | 1.6318 | 43.48 |
| | | 11 | Vertex | 7.8 | 0.5125 | 15.59 |
| | | 12 | Vertex | 8.0 | 0.4394 | 14.06 |
| Cormier (2011) | Circular | - | Frontal | 5.4 | 3.2 | 47.00 |

the inner surface of the skull with respect to the GHBMC head center of gravity (CG) node was sampled at 10 kHz as well.

The following protocol was used to group elements into coup and contre-coup regions of interest (ROI). First, a vector was computed between the brain CG and the impact location on the surface of the head. After this vector was established, a vector was calculated between each brain element and the brain CG. Taking advantage of the mathematical cross-product, the angle between the element vector and the impact location vector was computed. If the resulting angle was less than 60°, the element was included in the coup ROI. If the angle was greater than 120°, the element was included in the contre-coup ROI. These computations were performed for each impact target, resulting in six sets of coup and contre-coup ROIs across all experiments simulated. After sorting each element into either the coup ROI, contre-coup ROI, or neither, the peak maximum principal strain for each element in each ROI was stored in descending order. The 95th percentile of the maximum principal strain for both the coup and contre-coup ROIs in each impact were calculated.

In addition to the collection of brain element strain, a skull deflection metric was created and obtained for each simulation. The maximum skull deflection metric was developed to capture the furthest intrusion of any single node into the cranial space.

Linear regression analysis was performed between the skull deflection metric, input kinetic energy, and brain strain metrics. Brain strain metrics included 95th percentile maximum principal strain measured in the coup and contre-coup ROIs. Finally, a Wilcoxon signed ranked test was used to compare the median coup and contre-coup values of 95th percentile maximum principal strain measured in the simulations using $\alpha$ level 0.05.

## RESULTS

Nine experimental tests were simulated in this study. Input kinetic energies ranged from 14.06 to 110.94 J. Skull deflection ranged from 1.24-4.98 mm. 95th percentile coup and contre-coup ROI strain ranged from 0.008-0.08 and 0.0057-0.071, respectively.

Maximum skull deflection and kinetic energy were positively correlated with brain strain. The strongest correlation to 95th percentile maximum principal strain in the coup ROI was associated maximum skull deflection ($r^2$=0.79, p=0.0013, Figure 1), followed by kinetic energy ($r^2$=0.63, p=0.0112). Linear relationships were observed for contre-coup ROI 95th percentile strain as well: maximum skull deflection ($r^2$=0.90, p=0.0001), kinetic energy ($r^2$=0.81, p=0.0009).

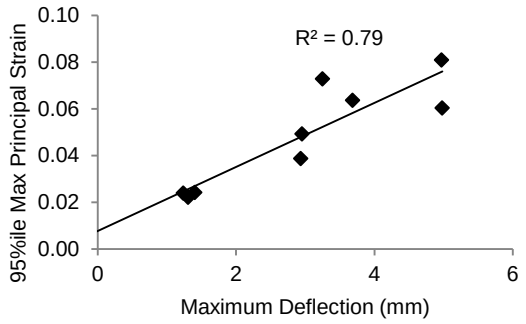


***Figure 1. 95th percentile maximum principal strain in the coup ROI linearly regressed against maximum skull deflection.***

The 95th percentile maximum principal strain in the coup and contre-coup ROI for every simulation are provided in Figure 2. In every simulation, the 95th percentile of maximum principal strain was higher in the coup ROI compared to the contre-coup ROI. Lower kinetic energy impacts and those impacts directed at the occipital bone produced the smallest differences in coup and contre-coup strain.

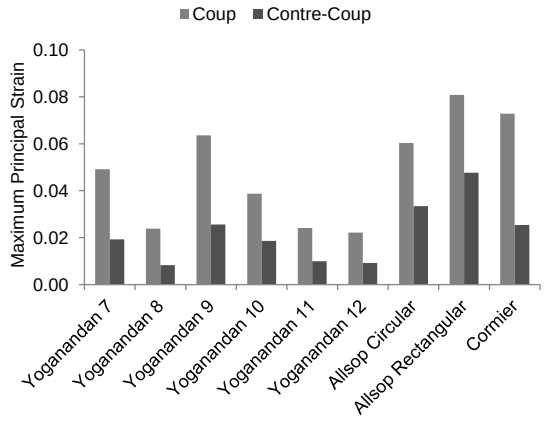


***Figure 2. 95th percentile maximum principal strain in the coup and contre-coup ROIs for matched impacts.***

There was a statistically significant difference between coup and contre-coup strain measures as assessed by Wilcoxon signed rank test (p-value < 0.05). On average, the coup ROI experienced 2.35 times higher 95th percentile maximum principal strain compared to contre-coup ROI.

**DISCUSSION**

The skull deformation metric developed in this study is pertinent to FE modeling of the head that cannot be directly measured through physical experimentation. Maximum skull deflection measurements provide a means to measure the effects of blunt head impact on local skull deformation and the resulting response of the brain. The exclusion of bulk head motion in these simulations accentuates the brain deformations resulting from local skull deformation separately from inertial effects.

The skull deformation metric was highly correlated with coup ROI 95th percentile maximum principal strain. This provides strong evidence to suggest that local skull deformation contributes to focal brain injuries. Further investigation into the role of skull deflection on brain injury response using the metric developed in this study as well as the continued development of other metrics is warranted for the prediction of underlying brain injury risk.

The difference between the strain distributions close to the impact compared to the distal locations is an important finding. It confirms the animal testing and pathophysiological findings in the literature that skull deformation contributes to brain injury [8, 27-29]. When examining the 95th percentile maximum principal strain distribution (Figure 2), the coup ROI always experienced higher strains than the contre-coup ROI. On average, the peak strain in the coup ROI of the brain reached 0.115±0.07. These values approach and sometimes exceed injurious thresholds for brain tissue strain [14]. This continues to confirm the injurious nature of skull deformation on the brain.

The ability to predict bony fracture through element erosion comes with the limitation that physical material is deleted from the model. In the higher energy impacts, we have observed element erosion that begins before the impactor transitions into the rebound phase. In this case, there is less material to resist the continued motion of the impactor into the cranial cavity. For this reason, the focus of this study was on those simulations without element erosion active in the model. However, the ability of element erosion methods to predict skull fracture should not be discounted as skull fracture alone is a moderate to severe injury [30].

One of the limitations of this study was the inability to capture the effects of skull fracture without eroding material in the model that would continue to absorb energy during an impact in the real-world. New technology would need to be developed in order to reach a balance between skull fracture detection and propagation and energy dissipation, while not deleting material from an FE model. Another limitation was the single impactor geometry used at each impact location. The implementation and simulation of each impactor geometry at each impact location would further elucidate impactor geometry versus impactor energy effects on strain distribution and skull deformation.

In previous literature, the terms coup and contre-coup are used to refer to proximal and distal regions of the brain with respect to impact location, but are not rigorously defined. The development of strict groupings of elements into these two ROIs based on quantifiable angles bolsters the work found here and ensures the results are repeatable. Furthermore, future studies using FE head models can use the same methodology to define coup and contre-coup ROIs in order to obtain consistent results.

## CONCLUSIONS

This study was conducted using the Global Human Body Models Consortium 50th percentile head model and simulated physical cadaveric experiments with no translational or rotational kinematics of the head CG in order to understand the relationship between skull deformation and brain response. One skull deformation metric was developed and employed to investigate its relationship with coup strain distribution. Nine experimental cases were reconstructed. Strict definitions of coup and contre-coup were employed. The difference between coup and contre-coup strain measures were also tested along with the correlations between a developed skull deformation metric and brain strain metrics.

Maximum skull deflection was correlated with 95th percentile maximum principal strain in the coup ROI of the brain model. There was a significant difference between coup and contre-coup 95th percentile strain ranging from 1.69-2.86 times higher across the simulations. Finally, this study demonstrated that strain profiles can be generated in the coup region of the brain in the absence of head CG rotational kinematics, which further justifies the need to study the role of skull deformation in head injury risk.

## ACKNOWLEDGEMENTS

Views expressed are those of the authors and do not represent the views of any sponsors. Funding for this project was provided by the National Highway Traffic Safety Administration under Cooperative Agreement Number DTNH22-10-H-00294. The M50-O v4.5 model was developed as part of the Global Human Body Models Consortium project. The authors acknowledge gratefully acknowledge the contributions of the Full Body Models COE at Wake Forest University (PIs, FS Gayzik, JD Stitzel) and the Head COE at Wayne State University (PI, L Zhang).

## REFERENCES

[1] C. A. Taylor, J. M. Bell, M. J. Breiding, and L. Xu, "Traumatic Brain Injury-Related Emergency Department Visits, Hospitalizations, and Deaths - United States, 2007 and 2013," *MMWR Surveill Summ,* vol. 66, pp. 1-16, Mar 17 2017.

[2] V. G. Coronado, L. Xu, S. V. Basavaraju, L. C. McGuire, M. M. Wald, M. D. Faul, B. R. Guzman, and J. D. Hemphill, "Surveillance for traumatic brain injury-related deaths--United States, 1997-2007," *MMWR Surveill Summ,* vol. 60, pp. 1-32, May 6 2011.

[3] J. M. Abel, T. A. Gennarelli, and H. Segawa, "Incidence and severity of cerebral concussion in the rhesus monkey following sagittal plane angular acceleration," SAE Technical Paper 0148-7191, 1978.

[4] R. Coimbra, C. Conroy, D. B. Hoyt, S. Pacyna, M. May, S. Erwin, G. Tominaga, F. Kennedy, M. Sise, and T. Velky, "The influence of damage distribution on serious brain injury in occupants in frontal motor vehicle crashes," *Accident Analysis & Prevention,* vol. 40, pp. 1569-1575, 2008.

[5] T. A. Gennarelli, "Mechanisms of brain injury," *J Emerg Med,* vol. 11 Suppl 1, pp. 5-11, 1993.

[6] E. S. Gurdjian, "Recent advances in the study of the mechanism of impact injury of the head--a summary," *Clinical neurosurgery,* vol. 19, pp. 1-42, 1972.

[7] G. S. Nusholtz, B. Wylie, and L. G. Glascoe, "Cavitation/boundary effects in a simple head impact model," *Aviation, space, and environmental medicine,* vol. 66, pp. 661-667, 1995.

[8] S. A. Shatsky, W. A. Alter, D. E. Evans, V. W. Armbrustmacher, G. Clark, and K. M. Earle,

"Traumatic distortions of the primate head and chest: correlation of biomechanical, radiological and pathological data," in *Proceedings: Stapp Car Crash Conference*, 1974.
[9] E. G. Takhounts, M. J. Craig, K. Moorhouse, J. McFadden, and V. Hasija, "Development of brain injury criteria (BrIC)," *Stapp Car Crash J*, vol. 57, pp. 243-66, Nov 2013.
[10] E. G. Takhounts, S. A. Ridella, V. Hasija, R. E. Tannous, J. Q. Campbell, D. Malone, K. Danelson, J. Stitzel, S. Rowson, and S. Duma, "Investigation of traumatic brain injuries using the next generation of simulated injury monitor (SIMon) finite element head model," *Stapp Car Crash J*, vol. 52, pp. 1-31, Nov 2008.
[11] A. A. Weaver, K. A. Danelson, and J. D. Stitzel, "Modeling brain injury response for rotational velocities of varying directions and magnitudes," *Ann Biomed Eng*, vol. 40, pp. 2005-18, Sep 2012.
[12] A. Holbourn, "Mechanics of head injuries," *The Lancet*, vol. 242, pp. 438-441, 1943.
[13] E. G. Takhounts, J. R. Crandall, and K. Darvish, "On the importance of nonlinearity of brain tissue under large deformations," *Stapp Car Crash J*, vol. 47, pp. 79-92, Oct 2003.
[14] E. G. Takhounts, R. H. Eppinger, J. Q. Campbell, R. E. Tannous, E. D. Power, and L. S. Shook, "On the Development of the SIMon Finite Element Head Model," *Stapp Car Crash J*, vol. 47, pp. 107-33, Oct 2003.
[15] J. E. Urban, C. T. Whitlow, C. A. Edgerton, A. K. Powers, J. A. Maldjian, and J. D. Stitzel, "Motor vehicle crash-related subdural hematoma from real-world head impact data," *J Neurotrauma*, vol. 29, pp. 2774-81, Dec 10 2012.
[16] J. E. Urban, C. T. Whitlow, and J. D. Stitzel, "Investigation of Intraventricular Hemorrhage Volume in Motor Vehicle Crash Occupants," *Trauma cases Rev*, vol. 1, 2015.
[17] N. Yoganandan, J. L. Baisden, D. J. Maiman, T. A. Gennarelli, Y. Guan, F. A. Pintar, P. Laud, and S. A. Ridella, "Severe-to-fatal head injuries in motor vehicle impacts," *Accid Anal Prev*, vol. 42, pp. 1370-8, Jul 2010.
[18] N. Yoganandan, T. A. Gennarelli, J. Zhang, F. A. Pintar, E. Takhounts, and S. A. Ridella, "Association of contact loading in diffuse axonal injuries from motor vehicle crashes," *J Trauma*, vol. 66, pp. 309-15, Feb 2009.
[19] L. E. Miller, J. E. Urban, and J. D. Stitzel, "Development and validation of an atlas-based finite element brain model," *Biomech Model Mechanobiol*, Jan 13 2016.
[20] A. K. Ommaya, A. E. Hirsch, E. S. Flamm, and R. H. Mahone, "Cerebral concussion in the monkey: an experimental model," *Science*, vol. 153, pp. 211-2, Jul 08 1966.
[21] F. S. Gayzik, D. P. Moreno, C. P. Geer, S. D. Wuertzer, R. S. Martin, and J. D. Stitzel, "Development of a full body CAD dataset for computational modeling: a multi-modality approach," *Ann Biomed Eng*, vol. 39, pp. 2568-83, Oct 2011.
[22] H. Mao, L. Zhang, B. Jiang, V. V. Genthikatti, X. Jin, F. Zhu, R. Makwana, A. Gill, G. Jandir, A. Singh, and K. H. Yang, "Development of a finite element human head model partially validated with thirty five experimental cases," *J Biomech Eng*, vol. 135, p. 111002, Nov 2013.
[23] D. L. Allsop, T. R. Perl, and C. Y. Warner, "Force/deflection and fracture characteristics of the temporo-parietal region of the human head," SAE Technical Paper 0148-7191, 1991.
[24] J. Cormier, S. Manoogian, J. Bisplinghoff, S. Rowson, A. Santago, C. McNally, S. Duma, and J. Bolte, "The tolerance of the frontal bone to blunt impact," *Journal of biomechanical engineering*, vol. 133, p. 021004, 2011.
[25] N. Yoganandan, F. A. Pintar, A. Sances, Jr., P. R. Walsh, C. L. Ewing, D. J. Thomas, and R. G. Snyder, "Biomechanics of skull fracture," *J Neurotrauma*, vol. 12, pp. 659-68, Aug 1995.
[26] GHBMC, "User Manual: M50 Occupant Version 4.5 for LS-DYNA," ed, 2016.
[27] T. A. Gennarelli, "Head injury in man and experimental animals: clinical aspects," in *Trauma and Regeneration*, ed: Springer, 1983, pp. 1-13.
[28] A. K. Ommaya, R. L. Grubb, Jr., and R. A. Naumann, "Coup and contre-coup injury: observations on the mechanics of visible brain injuries in the rhesus monkey," *J Neurosurg*, vol. 35, pp. 503-16, Nov 1971.
[29] G. S. Nusholtz, P. Lux, P. Kaiker, and M. A. Janicki, "Head impact response-Skull deformation and angular accelerations," in *Proceedings: Stapp Car Crash Conference*, 1984, pp. 41-74.
[30] AAAM, "Abbreviated Injury Scale, Update 2008," Association for Advancement of Automatic Medicine, Barrington, USA2008.